Iraqi Journal of Physics, 2022 *Vol.20, No. 3, PP. 40-49*
DOI: 10.30723/ijp.v20i3.1004
P-ISSN: 2070-4003
E-ISSN: 2664-5548

Calculation of the Magnetic Dipole and Electric Quadrupole Moments of some Sodium Isotopes using Shell Model with Skyrme Interaction

Ghofran. W. Harby[1a*] and Ali. A. Alzubadi[1b]
[1]*Department of Physics, College of Science, University of Baghdad, Baghdad, Iraq*
[b]E-mail: ali.kareem@sc.uobaghdad.edu.iq
[a*]Corresponding author: ghafranwaleed95@gmail.com

Abstract

In the present work, the magnetic dipole and electric quadrupole moments for some sodium isotopes have been calculated using the shell model, considering the effect of the two-body effective interactions and the single-particle potentials. These isotopes are; ^{21}Na (3/2+), ^{23}Na (3/2+), ^{25}Na (5/2+), ^{26}Na (3+), ^{27}Na (5/2+), ^{28}Na (1+) and, ^{29}Na (3/2+). The one-body transition density matrix elements (OBDM) have been calculated using the (USDA, USDB, HBUMSD and W) two-body effective interactions carried out in the *sd*-shell model space. The *sd* shell model space consists of the active $2s_{1/2}$, $1d_{5/2,}$ and$1d_{1/2}$ valence orbits above the inert ^{16}O nucleus core, which remains closed. Skyrme interaction was implemented to generate the single-particle matrix elements with Hartree-Fock approximation and compared with those of harmonic oscillator and Wood-Saxon potentials. From the outcome of our investigation, it is possible to conclude that the shell model calculations with Skyrme-type interaction give a reasonable description for most of the selected Na isotopes. No significant difference was noticed for the magnetic dipole moments and electric quadrupole moments with experimental data, where all signs for the experimental data are reproduced correctly.

Article Info.

Keywords:
Magnetic dipole moment, electric quadrupole moment, Skyrme interaction, shell model, effective interaction.

Article history:
Received: May 21, 2022
Accepted: Aug. 15, 2022
Published: Sep. 01,2022

1. Introduction

The magnetic dipole (μ) and electric quadrupole (Q2) moments are considered one of the most important ways to learn about the nuclear structure and obtain dense and deep information like deformations, charge, and nuclear moments in this field [1]. The magnetic dipole moments of nuclei are sensitive to the orbits occupied by the valence nucleons. They offer a perfect test of the purity of a specific configuration mixing shell model [2]. The electric quadrupole and magnetic dipole moments can assist us in understanding some aspects of the nuclear structure.

On the other hand, electromagnetic moments are considered one of the most basic probes for obtaining information on the nuclear structure across the entire nuclear chart [3, 4]. Nuclear deformation can affect the shell structure of single-particle levels in a spherical potential [5]. The shell model has been successful in describing nuclei near magic numbers. However, it fails to describe the structure of nuclei with many valence nucleons outside closed shells, where the residual interactions between such nucleons' deformation are the most significant and essential consequences [6]. This model has shortcomings, particularly true for heavier nuclei [7]. We have already seen that the shell model does not predict magnetic dipole moments or the spectra of excited states very well [8]. The nuclear shell model has been applied to the properties of nuclei near stability and how its applications are extended to nuclei out to the proton and neutron drip lines. The nuclear electric quadrupole moment is considered a probe for the deviation of nuclear charge from spherical symmetry, which gives a valuable measure of how the core is polarized, especially if the valence nucleons are neutrons that do not directly participate in the electric quadrupole moment [9]. According to the convention, the value of electric quadrupole moments is positive if the ellipsoid is prolate and negative if it is oblate. It is

the simplest deformation and one of the significant quantities that limit the shape of the nucleus [10].

The present work aims to calculate the magnetic dipole and electric quadrupole moments for some sodium isotopes using the shell model, considering the effect of the two-body effective interactions and the single-particle potentials. The *sd* shell model space will be used for this purpose, consisting of the active $2s_{1/2}$, $1d_{5/2}$ and$1d_{1/2}$ valence orbits above the inert ^{16}O nucleus core, which remains closed.

2. Theoretical consideration

The electric 2^L pole operator $r^L Y_{LM}(\hat{r})$ possesses parity $(-1)^L$and the electric 2^L pole moment should vanish for odd values of L. The intrinsic is defined with respect to the charge distribution axis of symmetry. The sum of the products of the one-body density matrix (OBDM) times the single-particle matrix elements is the nuclear matrix element of the electromagnetic ($\hat{O}$) and electron scattering ($\hat{T}$) operators between the initial *I* and final (*f*) nuclear states for certain multipolarity [11]:

$$\langle f \| \hat{X}(\lambda)_{t_z} \| i \rangle = \sum_{k_a k_b} OBDM(fik_ak_b\lambda) \langle k_a \| \hat{X}(\lambda)_{t_z} \| k_b \rangle \quad (1)$$

The electromagnetic operator ($\hat{O}$) and the electron scattering operator ($\hat{T}$) are represented by the $\hat{X}$ operator. *k* represents the single-particle states (*nlj*). The OBDM is determined by:

$$OBDM(fik_ak_b\lambda) = \frac{\langle f \| \left[a^+_{k_a} \otimes \tilde{a}_{k_b}\right]^{\lambda} \| i \rangle}{\sqrt{2\lambda+1}} \quad (2)$$

All the quantum numbers required to differentiate the states are included in *I* and *f*. In terms of the M1 operator, the magnetic dipole moment is defined as [12]:

$$\mu = \sqrt{\frac{4\pi}{3}} \begin{pmatrix} J & J & J \\ -J & 0 & J \end{pmatrix} \sum_{t_z} \langle J \| \hat{O}(M1)_{t_z} \| J \rangle \mu_N \quad (3)$$

where $\langle J \| \hat{O}(M1)_{t_z} \| J \rangle$ is the operator of the magnetic transition, and $\mu_N$is the nuclear magneton $\mu_N = \frac{e\hbar}{2m_p c} = 0.1051$ efm, with m_p the proton mass. The orbital and spin free nucleon *g* factors *g*(free) are: $g_l^p = 1$, $g_s^p = 5.585$ for proton and$g_l^p = 0$, $g_s^p = -3.826$ for neutron [12].

The electric quadrupole moment is defined in terms of the E2 operator as:

$$Q = \sqrt{\frac{16\pi}{5}} \begin{pmatrix} j_i & 2 & j_i \\ -j_i & 0 & j_i \end{pmatrix} \sum_{t_z} \langle J \| \hat{O}(E2)_{t_z} \| J \rangle e_{t_z} \quad (4)$$

where $|J\rangle$ includes all the quantum numbers needed to differentiate the nuclear states in the initial and final nuclear states. The Skyrme potential is employed for the central potential; it is a two-body interaction. In the Hartree-Fock (HF) approximation, it may be used to construct a one-body potential [13]. It is a mean-field potential, and it is designed to mimic the realistic nucleon-nucleon (and nucleon-nucleon-nucleon) forces by providing the mean-field due to all the nucleons that make up the nucleus. The Skyrme potential V_{skyrme}can be written as [14]:

$$V_{Skyrme}(\vec{r}_1,\vec{r}_2) = t_0(1+x_0\hat{P}_\sigma)\delta_{12} + \frac{t_1}{2}(1+x_1\hat{P}_\sigma)\left[\vec{k}'^2\delta_{12} + \delta_{12}\vec{k}^2\right]$$
$$+ t_2(1+x_2\hat{P}_\sigma)\vec{k}'\delta_{12}\vec{k} + \frac{t_3}{6}(1+x_3\hat{P}_\sigma)\rho\left(\frac{\vec{r}_1+\vec{r}_2}{2}\right)^\alpha \delta_{12} + iW_0\,\vec{k}'\delta_{12}(\vec{\hat{\sigma}}_1+\vec{\hat{\sigma}}_2)\times\vec{k}$$
$$+ \frac{t_e}{2}\left(\left[3\,(\vec{\hat{\sigma}}_1.\vec{k}')\,(\vec{\hat{\sigma}}_2.\vec{k}') - (\vec{\hat{\sigma}}_1.\vec{\hat{\sigma}}_2)\vec{k}'^2\right]\delta_{12} + \delta_{12}\left[3(\vec{\hat{\sigma}}_1.\vec{k})\,(\vec{\hat{\sigma}}_2.\vec{k}) - (\vec{\hat{\sigma}}_1.\vec{\hat{\sigma}}_2)\vec{k}^2\right]\right)$$
$$+ t_0\left[3(\vec{\hat{\sigma}}_1.\vec{k})\delta_{12}(\vec{\hat{\sigma}}_2.\vec{k}) - (\vec{\hat{\sigma}}_1.\vec{\hat{\sigma}}_2)\vec{k}'\delta_{12}\vec{k}\right] \quad \textbf{(5)}$$

where $\delta_{12} = \delta(\vec{r}_1 - \vec{r}_2)$ and $\hat{k}$, $\hat{k}'$ are the relative momentum operators with $\hat{k}$ acting on the right, while $\hat{k}'$ is the operator acting on the left and given by:

$$\hat{\boldsymbol{k}} = \frac{\mathbf{1}}{\mathbf{2}\boldsymbol{i}}(\overrightarrow{\boldsymbol{\nabla}_\mathbf{1}} - \overrightarrow{\boldsymbol{\nabla}_\mathbf{2}}), \quad \hat{\boldsymbol{k}}' = -\frac{\mathbf{1}}{\mathbf{2}\boldsymbol{i}}(\overrightarrow{\boldsymbol{\nabla}_\mathbf{1}} - \overrightarrow{\boldsymbol{\nabla}_\mathbf{2}}) \quad \textbf{(6)}$$

and $\hat{P}_\sigma$ is the spin-exchange operator that is given as:

$$\hat{\boldsymbol{P}}_{\boldsymbol{\sigma}} = \frac{\mathbf{1}}{\mathbf{2}}(\mathbf{1}+\hat{\boldsymbol{\sigma}}_\mathbf{1}.\hat{\boldsymbol{\sigma}}_\mathbf{2}) \quad \textbf{(7)}$$

3. Result and discussion

In the present work, the nuclear shell model calculations are performed using the NuShellX@MSU shell model code [15]. It uses a *J* -coupled proton-neutron basis, and *J* -scheme matrix dimensions of up to 100 million can be considered. The radial wave functions of the single-particle matrix elements were calculated using a two-body Skyrme interaction potential and the HO and WS. Discussion of the results will be divided into three sections; the first is devoted to the magnetic dipole moment, the second section examines the electric quadrupole moments, followed by the conclusions section.

3.1. Magnetic dipole moment

The calculation of magnetic dipole moments of Na isotopes in *sd* model space using four two-body effective interactions; USDA, USDB, HBUMSD and W, with free nucleon g factors. The calculated results are presented in Table 1 compared to the experimental data from Ref. [16, 17]. The previously displayed values show that the calculated magnetic dipole moments are in good agreement with the experimental data provided [16, 17]. For more illustration, the comparison of the calculated μ moments with the corresponding experimental data is depicted in Figs. 1 and 2. It is obvious that the HBUMSD interaction gives results that are broadly consistent with experimental data.

Table 1: Theoretical calculated of magnetic dipole moments μ (nm) for Na-isotopes using four two-body effective interactions; USDA, USDB, HBUMSD and W in comparison with the experimental data from Ref [16, 17].

Mass No.	J^{π}	USDA	USDB	HBUMSD	W	Exp
21	3/2+	2.472	2.478	2.555	2.502	2.386
23	3/2+	2.139	2.128	2.311	2.194	2.217
25	5/2+	3.562	3.563	3.733	3.662	3.683
26	3^{+}	2.837	2.852	2.879	2.878	2.851
27	5/2+	3.829	3.833	3.832	3.828	3.895
28	1^{+}	2.366	2.218	2.48	2.33	2.426
29	5/2+	2.506	2.544	2.528	2.52	2.449

To achieve the better results, the applicability of the present method is tested in calculating the moments using different single-particle potentials and two-body effective interaction HBUMSD. Namely, the harmonic oscillator (HO), Woods Saxon (WS), and Skyrme Hartree-Fock (SHF) with SLy4 parameterization. From Table 2 and Figs. 3 and 4, it is clear that the calculated results using these types of potentials are in good agreement with the experimental data of magnetic dipole moments. In contrast, ^{26}Na isotope gives the best and closest result to the experimental data [16, 17].

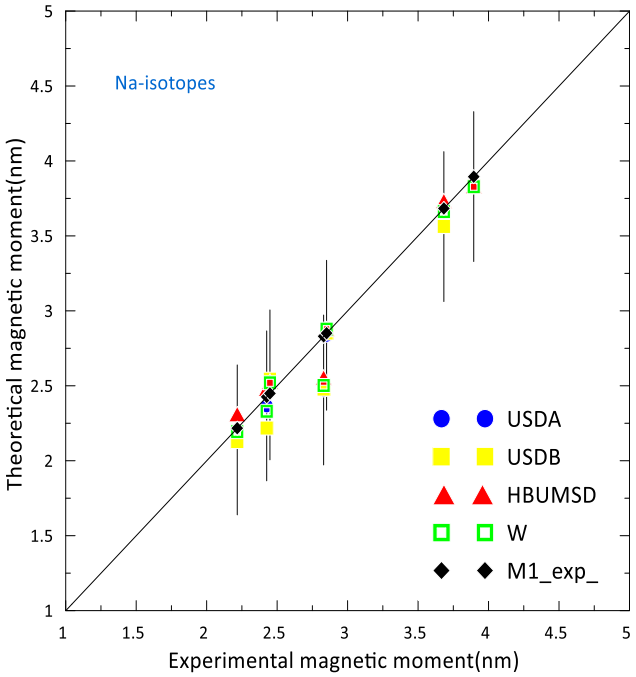

Figure 1: Comparison between theoretical magnetic moments μ (nm) and experimental data [16, 17] for Na-isotopes using two-body effective interactions; USDA, USDB, HBUMSD and W.

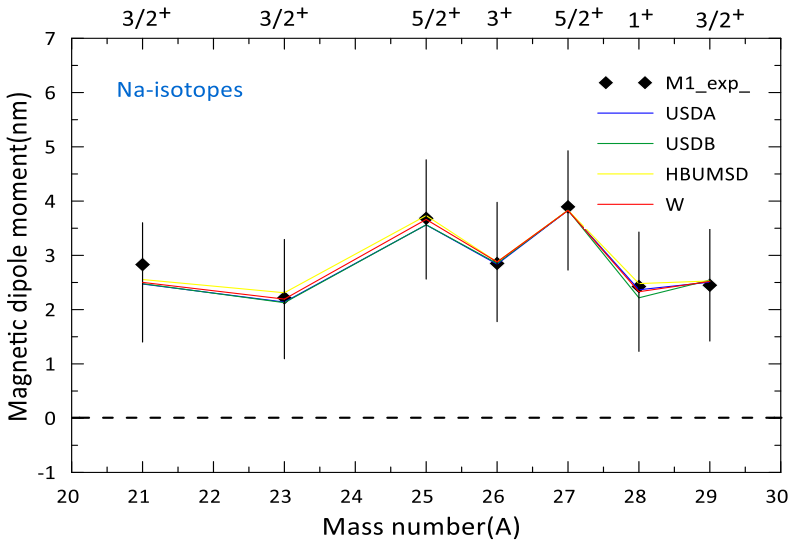

Figure 2: The calculated magnetic dipole moments μ (nm) for Na-isotopes using different two-body effective interactions in comparison with the experimental data of Refs. [16, 17].

Table 2: Theoretical calculated magnetic dipole moments μ (nm) for Na-isotopes using three different single-particle potentials; HO, WS, and SLy4 in comparison with experimental data from Refs. [16, 17].

Isotopes	J^{π}	HO	SLy4	WS	Exp
21	3/2+	2.489	2.489	2.489	2.386
23	3/2+	2.098	2.098	2.098	2.217
25	5/2+	3.367	3.367	3.367	3.683
26	3^{+}	2.632	2.632	2.632	2.851
27	5/2+	3.647	3.647	3.647	3.895
28	1^{+}	2.081	2.081	2.081	2.426
29	5/2+	2.438	2.438	2.438	2.449

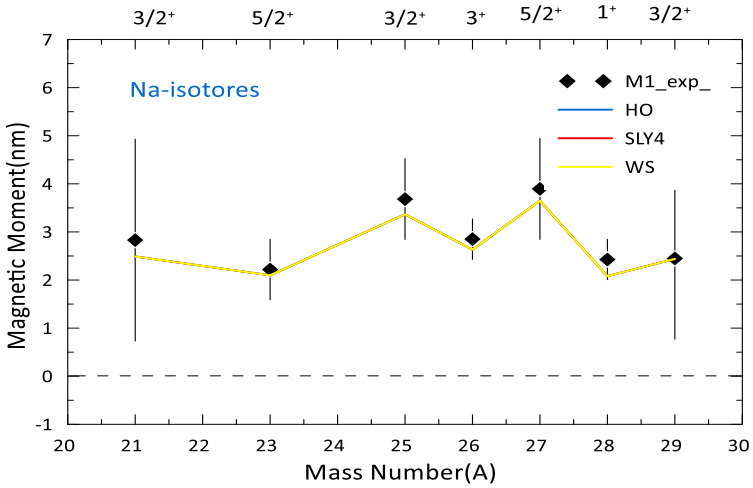

Figure 3: The calculated magnetic dipole moments μ (nm) for Na-isotopes using different single-particle potentials in comparison with the experimental data of Refs. [16, 17].

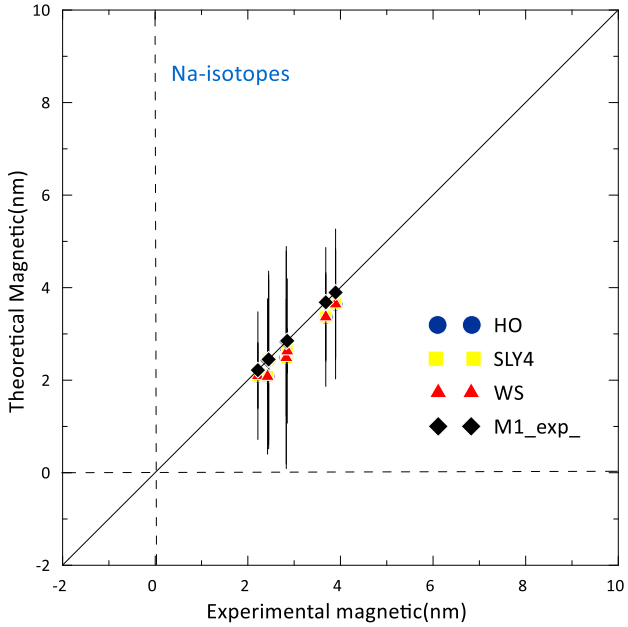

Figure 4: The calculated magnetic dipole moments μ (nm) vs the experimental data [16, 17] for Na-isotopes using different single-particle potentials; HO, WS, and SLy4.

3.2. Electric quadrupole moments

The electric quadrupole moments of Na isotopes are calculated and shown in Table 3 and Figs. 5 and 6. The electric quadrupole moments for isotopes are calculated with two-body effective interactions of *sd* model space MS and compared with the available experimental data from Ref [16, 17]. It is clear that the calculations with *sd* wave functions reasonably explain the experimental data and predict the correct sign of the prolate deformation for the isotopes ^{21}Na, ^{23}Na, and ^{29}Na and oblate deformation for ^{26}Na and ^{27}Na isotopes. The USDA and USDB interactions failed to reproduce the correct sign for the ^{25}Na isotope. As in the case of magnetic dipole moments, to achieve the best results, we test the applicability of the present method in calculating the electric quadrupole moments using different single-particle potentials, namely; the HO, WS, and SLy4. As shown in Table 4 and Figs. 7 and 8, the calculated *Q2* results are not very sensitive to changing the potentials compared to the experimental data [16,17], where we have good agreement.

Table 3: The calculated electric quadrupole moments in e^2fm^2 for Na-isotopes using different two-body effective interactions; USDA, USDB, HBUMSD and W in comparison with experimental data from Refs. [16, 17].

Mass no.	J^π	USDA	USDB	HBUMSD	W	Q(Exp)
21	3/2+	12.66	11.05	11.95	11.14	12.4
23	3/2+	10.89	10.7	12.02	11.04	10.4
25	5/2+	0.31	0.22	-0.51	-0.36	-10
26	3^+	-0.49	-0.46	-0.52	-1.16	-0.53
27	5/2+	-1.04	-1.15	-1.56	-1.43	-0.7
28	1^+	4.58	4.5	4.36	4.21	3.95
29	3/2+	7.14	7.19	7.27	6.93	8.50

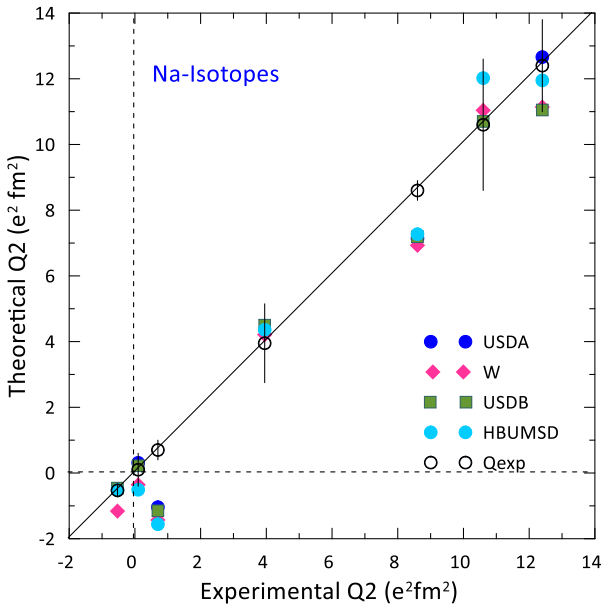

Figure 5: The calculated electric quadrupole moments Q2 (e^2fm^2) vs the experimental data [16, 17] for Na-isotopes using different two-body effective interactions; USDA, USDB, HBUMSD and W.

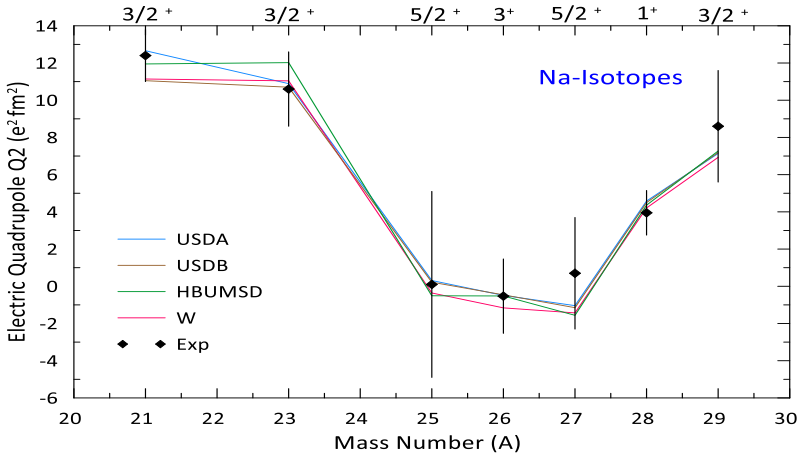

Figure 6: The calculated electric quadrupole moments Q2 (e^2fm^2) vs mass number (A) for Na-isotopes using different two-body effective interactions compared to the experimental data of Refs. [16, 17].

Table 4: The theoretical calculated electric quadrupole moments in e^2fm^2 for Na-isotopes using three different single-particle potentials; HO, WS, and SLy4 in comparison with experimental data taken from Refs. [16, 17].

Mass no.	J^π	HO	SLY4	WS	Q(Exp)
21	3/2+	10.94	11.69	11.69	12.4
23	3/2+	10.67	10.720	10.720	10.4
25	5/2+	0.3503	0.3383	0.3383	-10.0
26	3^+	-0.417	-0.4027	-0.4027	-0.53
27	5/2+	-1.214	-1.164	-1.164	-0.7
28	1^+	4.397	4.282	4.282	3.95
29	3/2+	6.949	6.692	6.692	8.50

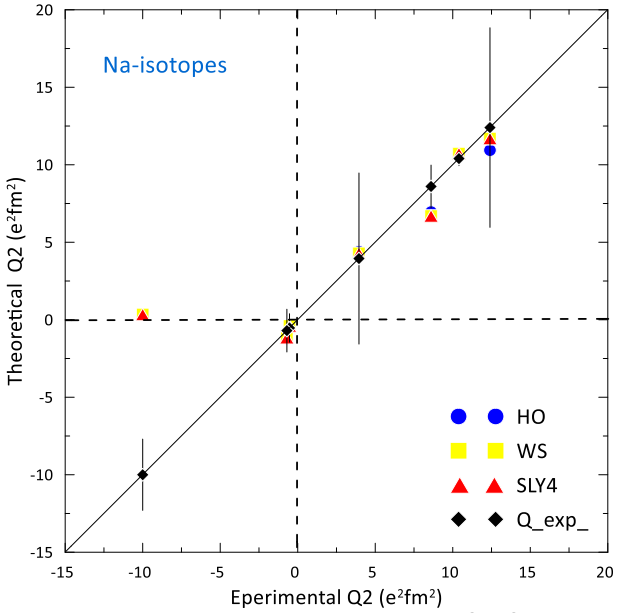

Figure 7: The calculated electric quadrupole moments Q2 (e^2fm^2) vs the experimental data [16, 17] for Na-isotopes using different single-particle potentials; HO, WS, 89and SLy4.

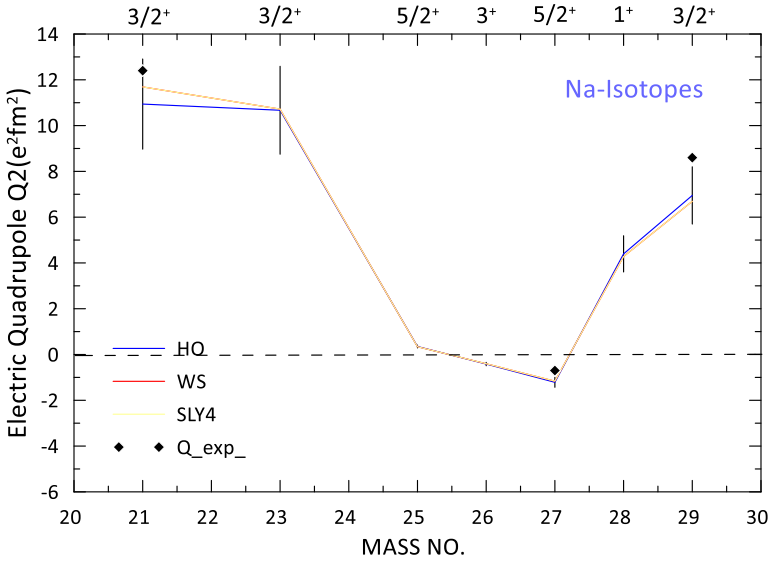

Figure 8: The calculated electric quadrupole moments Q2 (e^2fm^2) for Na-isotopes using different single-particle potentials compared to the experimental data of Refs. [16, 17].

4. Conclusions

The magnetic dipole and electric quadrupole moments for Na isotopes have been calculated in *sd* shell model space, considering the sensitivity for changing the two-body effective interactions and the single-particle potentials. All the calculated results have also been compared with available experimental data. From the outcome of our investigation, it is possible to conclude that the shell model calculations in *sd* model space with Skyrme type interaction give a reasonable description for most of the selected Na isotopes. No significant difference was noticed for the magnetic dipole moments μ and electric quadrupole moments *Q2* with experimental data, where all signs for the experimental data are reproduced correctly, where it was found that ^{26}Na isotope gives the best result and the closest to the experimental data. It is obvious that the HBUMSD interaction gives results

that are broadly consistent with experimental data. The present work provides more information on previously known spectroscopic properties by implementing the shell model calculations with mean-field potential.

Acknowledgements

The authors would like to thank Prof. Dr B. A. Brown from Michigan State University for providing the shell model code NuShellX@MSU.

Conflict of interest

Authors declare that they have no conflict of interest.

References

1. Ali A.H. and Alzubadi A.A., *Calculation magnetic dipole moments, electric quadrupole moments and form factors for some Ti isotopes.* Physica Scripta, 2020. **95**(10): pp. 105306.
2. Maison D.E., Skripnikov L.V., and Flambaum V.V., *Theoretical study of ^{173}YbOH to search for the nuclear magnetic quadrupole moment.* Physical Review A, 2019. **100**(3): pp. 032514(1-5).
3. Keim M., Georg U., Klein A., Neugart R., Neuroth M., Wilbert S., Lievens P., Vermeeren L., and Brown B., *Measurement of the electric quadrupole moments of $^{26-29}$Na.* The European Physical Journal A, 2000. **8**(1): pp. 31-40.
4. Brown B.A., *The nuclear shell model towards the drip lines.* Progress in Particle Nuclear Physics, 2001. **47**(2): pp. 517-599.
5. Hadyńska-Klęk K., Napiorkowski P.J., Zielińska M., Srebrny J., Maj A., Azaiez F., Dobón J.V., Kicińska-Habior M., Nowacki F., and Naïdja H., *Quadrupole collectivity in ^{42}Ca from low-energy Coulomb excitation with AGATA.* Physical Review C, 2018. **97**(2): pp. 024326(1-20).
6. Lawson R., *Theory of the nuclear shell model*. 1980, New York Oxford University Press.
7. Faessler A., *IBA and the Bohr-Mottelson model.* Nuclear Physics A, 1983. **396**: pp. 291-305.
8. Evans R.D. and Evans R., *The atomic nucleus*. Vol. 582. 1955: McGraw-Hill New York.
9. Neyens G., *Nuclear magnetic and quadrupole moments for nuclear structure research on exotic nuclei.* Reports on Progress in Physics, 2003. **66**(4): pp. 633-689.
10. Rainwater J., *Nuclear energy level argument for a spheroidal nuclear model.* Physical Review, 1950. **79**(3): pp. 432-434.
11. Safronova M., Safronova U., Radnaev A., Campbell C., and Kuzmich A., *Magnetic dipole and electric quadrupole moments of the ^{229}Th nucleus.* Physical Review A, 2013. **88**(6): pp. 060501(1-5).
12. Radhi R., Alzubadi A.A., and Ali A., *Magnetic dipole moments, electric quadrupole moments, and electron scattering form factors of neutron-Rich sd−pf cross-shell nuclei.* Physical Review C, 2018. **97**(6): pp. 064312(1-13).
13. Brussaard P.J. and Glaudemans P.W.M., *Shell model applications in nuclear spectroscopy*. 1977, Amsterdam: North Holland.
14. Brink D. and Stancu F., *Evolution of nuclear shells with the Skyrme density dependent interaction.* Physical Review C, 2007. **75**(6): pp. 064311(1-14).
15. Brown B. and Rae W., *The shell-model code NuShellX@ MSU.* Nuclear Data Sheets 2014. **120**: pp. 115-118.
16. *National Nuclear Data Center*: www-nds.iaea.org.
17. Stone N., *Table of nuclear magnetic dipole and electric quadrupole moments.* Atomic Data Nuclear Data Tables, 2005. **90**(1): pp. 75-176.

حساب العزوم ثنائية القطب المغناطيسيه ورباعية القطب الكهربائية لبعض نظائر الصوديوم باستخدام نموذج القشرة مع تفاعل سكيرم

غفران وليد حربي[1]، علي عبد اللطيف كريم[1]
[1]قسم الفيزياء، كلية العلوم، جامعة بغداد، بغداد، العراق

الخلاصة

تم حساب عزوم ثنائي القطب المغناطيسي و رباعي القطب الكهربائي لبعض نظائرالصوديوم باستخدام نموذج القشرة مع مراعاة تأثير التفاعلات ثنائية الجسيم الفعالة وكذلك جهد الجسيم المنفرد .هذه النظائر هي ^{21}Na (3/2+), ^{23}Na (3/2+), ^{25}Na (5/2+), ^{26}Na (3+), ^{27}Na (5/2+), ^{28}Na (1+) , ^{29}Na (3/2+). تم حساب عناصر المصفوفة للجسم المنفرد(OBDM) باستخدام التفاعلات ثنائية الجسيم الفعالة USDA, USDB, HBUMSD وW في فضاء الانموذج *sd*-shell. يتكون الانموذج من اوربيتالات التكافؤ النشطة $2s_{1/2}$, $1d_{5/2}$ و $1d_{1/2}$ والقلب الخامل ^{16}O والذي يكون دائما مغلق .تم أستخدام تفاعل سكيرم لتوليد عناصر المصفوفة احادية الجسيم مع تقريب هارتري-فوك ومقارنتها مع جهد المذبذب التوافقي وجهد وود-ساكسون. من نتيجة تحقيقنا، من الممكن أن نستنتج أن حسابات نموذج القشرة مع تفاعل من نوع سكيرم تعطي وصفًا معقولًا لمعظم نظائر الصوديوم المختارة. لم يلاحظ أي فرق مؤثر للعزوم ثنائي القطب المغناطيسية والرباعية الكهربائية مع البيانات التجريبية ، حيث يتم استنساخ جميع اشارات البيانات التجريبية بشكل صحيح.